Available online at www.sciencedirect.com

ScienceDirect

Energy Procedia 120 (2017) 254–261

Energy Procedia

www.elsevier.com/locate/procedia

INFUB - 11th European Conference on Industrial Furnaces and Boilers, INFUB-11

Numerical Study on the Influence of Operational Settings on Refuse Derived Fuel Co-firing in Cement Rotary Kilns

Liedmann B.[a*], Wirtz S.[a], Scherer V.[a], Krüger B.[b]

[a] *Department of Energy Plant Technology (LEAT), Ruhr-University, Bochum,*
[b] *Fraunhofer Institute for Environmental, Safety, and Energy Technology UMSICHT, Oberhausen*

Abstract

Cement production in rotary kilns requires large amounts of thermal energy, which is provided by combustion of different fuels. Substitution of fossil fuels by refuse derived fuels (RDF) can minimize production costs and reduce CO_2 emissions, but often causes displacement of the sintering zone, impacts flame stability and cement quality. The current paper briefly introduces our numerical approach which describes particle motion and combustion characteristics of typical non-spherical RDF particles. By using these models in CFD simulations, a case study is presented. Fuel properties, primary- and secondary air settings and fuel feed location for a generic rotary kiln of industrial scale are varied to show the effects of operational settings on co-firing of RDF. Shift of flame shape and location as well as particle burnout are analyzed. Based on the information generated, optimized operational settings are identified and discussed.

© 2017 The Authors. Published by Elsevier Ltd.
Peer-review under responsibility of the organizing committee of INFUB-11

Keywords: rotary kiln; cement clinker; CFD; combustion; refuse derived fuels (RDF); burner settings

1. Introduction

Rotary kilns are widely used for the production of cement clinker. The clinker formation process demands large amounts of thermal energy to heat up the material to sintering temperatures above 1700 K. To provide the energy required, different types of fossil and alternative fuels are commonly fired through the main burner at the material outlet of the kiln (see Fig. 1). Modern kiln burners are often so called multi-channel burners which consist of a number

* Corresponding author. Tel.: +49-234-32-26326; fax: +49-234-32-14227.
E-mail address: liedmann@leat.rub.de

1876-6102 © 2017 The Authors. Published by Elsevier Ltd.
Peer-review under responsibility of the organizing committee of INFUB-11
10.1016/j.egypro.2017.07.176

of different primary air and fuel conveyance ducts, allowing the combustion of different types of solid, liquid and gaseous fuels.

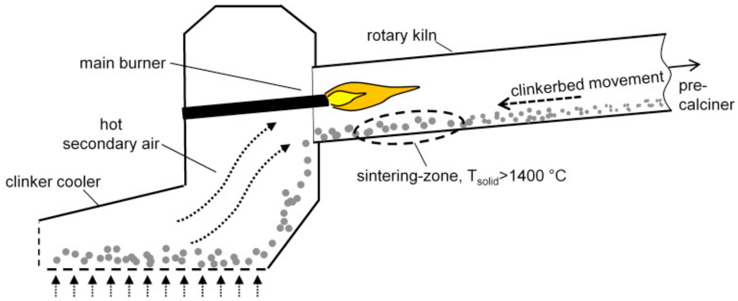

Fig. 1: Clinker formation process in a modern plant rotary kiln.

Additional energy is provided by secondary air, which recuperates heat in the clinker cooler and enters the kiln as a parallel stream around the burner.

Fossil fuels, typically pulverized coal, are increasingly replaced by refuse derived fuels (RDF) [1] which offer the potential to minimize production costs and to reduce CO_2-emissions. In contrast to fossil fuels, RDF consists of irregular shaped, mostly flat particles with edge lengths exceeding 1 cm. Large particle sizes and strong chemical and physical inhomogeneities hinder easy substitution of fossil fuels in rotary kilns [2] and limit their share at a low level [1]. The local heat release which is critical for flame geometry and temperature distribution is not just strongly dependent on the fuel properties but can also be influenced by primary- and secondary air settings [3]. According to this, a proper selection of these parameters offers potential to actively adjust the flame characteristics for RDF co-firing and gives the opportunity to obtain an appropriate RDF burnout. As general guidelines are rare and not profound, further research is needed to identify the effects of different operational points on heat distribution and fuel burnout in rotary kilns.

In this paper we present a case study of RDF co-firing in an industrial scale rotary kiln under different operational settings, regarding primary and secondary air variations as well as different RDF feed locations. For this study our in-house RDF flight and combustion models [4,5] were used in combination with Ansys FLUENT following the Euler/Lagrange approach.

2. Overview of the RDF Simulation Methodology

Our modelling approach is based on comprehensive fuel characterisation and numerical models, which were developed to calculate particle trajectories [4] and characteristic combustion behaviour [5] of the different RDF components.

2.1. Fuel characterisation

As a first step, a sorting analysis of an RDF sample is carried out, which groups the numerous fuel components into the major fractions (which shares are usually > 5 mass-%). For the case study in this paper, we assume a “model RDF” with typical components as shown in Figure 2. Major components usually are 3D plastics, 2D foil sheets, paper and cardboard (P&C) snippets, textiles and the fines representing the leftovers which cannot be assigned clearly to a particular fraction. Each of these fractions is extensively characterized by determining their thermophysical and calorific properties as well as geometrical parameters like particle shape and particle size distribution. Further experimental characterization is carried out to analyse individual particle trajectories in an automated drop-shaft [4] to obtain drag and lift coefficients and their time-dependent fluctuations. Characteristics of the thermal conversion process are investigated using a single particle reactor [6]. A single particle is suddenly introduced into a hot gas flow with temperatures up to 1200 °C and with varying oxygen concentration. Optical access through two ports allows analysis of the thermal conversion progress by video screening. Quantitative data measured are time scales of melting, decomposition, volatile combustion, char burn-out and the change of particle shape.

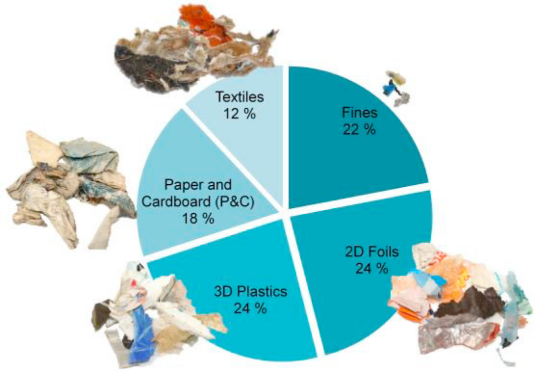

Fig. 2. Mass distribution of the model RDF and typical appearance of particles.

In order to avoid repetitions of fuel analyses, a comprehensive RDF database has been established and continually expanded. As numerous analyses have shown, it provides a good transferability among different RDFs for the specific material fractions.

2.2. Modelling Trajectories and Combustion of RDF Particles

Flight and combustion behaviour of large non-spherical RDF particles are different compared to classical fossil fuels (pulverized coal) which can be simplified as mass points. For that reason, simulations of RDF combustion require specific numerical models for particle motion and thermal conversion. Calculating the particle trajectories of flat non-spherical particles, the rotation and the torques resulting from the acting forces must be taken into account. These torques lead to the characteristic tumbling motion of the particles, which creates a fluctuating relative velocity between the gas phase and the particles. In order to describe the particle motion sufficiently, the resulting forces (drag force, lift force and gravitational force) and resulting torques acting on the particles are calculated. Lift- and drag-coefficients derived in the drop shaft experiments are applied to the calculations. As soon as the particle shape changes due to its combustion process, the drag coefficient is obtained from an adjusted correlation by Hölzer & Sommerfeld [7].

Table 1. Applied combustion laws.

Conversion Process	**Char-forming fractions (Textiles, P&C, Fines)**	**Non-char-forming fractions (3D Plastics, 2D Foils)**
I	Inert Heating	Inert Heating
II	Drying I (inner particle drying)	Drying II (surface drying)
III	Pyrolysis (constant particle shape)	Melting (change in particle shape)
IV	Char-Burnout	Decomposition

In the combustion model, a distinction is made between synthetic, non-char-forming polymers and biogenic, ligno-cellulosic materials. Table 1 shows the assignment of difference conversion laws to the main material fractions. For ligno-cellulosic materials (char forming), drying, pyrolysis and char-combustion were modelled in accordance with the models known for coal combustion [9,10]. Since drying and pyrolysis of large particles are limited by the heat conduction into the particle interior, they have been described through a multi-shell model for the temperature front progressing into the particle. For the subsequent heterogeneous combustion, the combustion rate is calculated as the effective value of the chemical reaction and the diffusion rate of the oxidant to the reactive surface. For non-char-forming particles (evaporating plastics) the phase transitions between solid, liquid and gas phase have to be considered.

The conversion model is based on the work of Bluhm-Drehnhaus [11], where the melting process and the chemical decomposition are determined in parallel using global conversion rates. The conversion rates depend on the respective phase quantities and the temperature profile within the particle. The progress of the melting process also controls the change in shape of the particle.

3. Simulations of the Rotary Kiln

CFD simulations were carried out for multiple operation points, varying primary and secondary air as well as fuel feed location and particle size. The results can be compared with pre-defined requirements (reference cases) for flame structure and temperature distribution, to better asses the effect of the changes.

3.1. Plant Description

The generic rotary kiln simulated is 40-meter-long, 4 meter in diameter and inclined by 2 degrees. The rotary kiln is equipped with a typical high-momentum multi-channel burner which injects solid RDF through a central duct (Fig. 3). Pulverized lignite is fed by a co-axial ring channel. Both RDF and lignite are transported by conveying air. Primary air is delivered as jet-air and swirling air. Secondary air is preheated in the clinker cooler (see Fig. 1) and flows around the burner into the rotary kiln. The rotary kiln volume is discretised with approx. 3 million hexahedral cells with a high spatial resolution in the near burner region. The solid material passing the kiln is approximated by a static bed aligned with a dynamic angle of repose of 30 degrees.

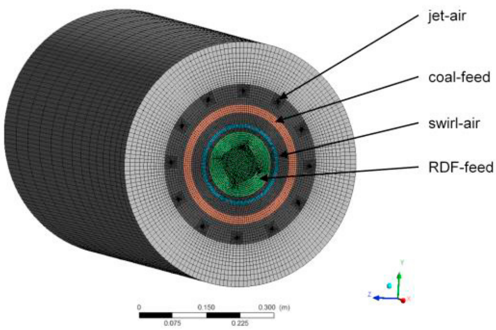

Fig. 3: Illustration of the (meshed) burner used for the study.

3.2. Models and Boundary Conditions

The simulations of the rotary kiln are performed using ANSYS Fluent with a discrete phase model implementing the RDF motion and combustion models described. For the turbulent flow the standard k-ε turbulence model is chosen, radiation is modelled by the P1-model, and for the combustion in the gaseous phase the Eddy-Dissipation model is applied. For the thermal boundary condition of the clinker bed, a typical, fixed temperature profile is set as shown in Figure 4. Heat loss through the kiln shell is calculated by heat conduction through the refractory-lined kiln tube. Particles falling onto the clinker bed are set to stay in place while conversion processes continue (except char burnout as oxygen is assumed to be zero in the clinker bed).

To be able to apply correct boundary conditions for the secondary air inflow from the clinker cooler, the system was simulated incorporating the clinker cooler once. The velocity profile at the clinker-outlet (secondary air inlet) has been stored and is set as inflow boundary in the subsequent combustion simulations. A simulation with mere pulverized lignite (LCV=22 MJ/kg) as primary fuel is designated as the first reference case (Case 0) for later comparisons of flame shape and temperature distribution. For the co-firing simulations, the fuel shares were chosen to be 64 % lignite and 36 % RDF of the total thermal heat input. The composition and some properties of the RDF fractions used in the simulations are shown in Table 2.

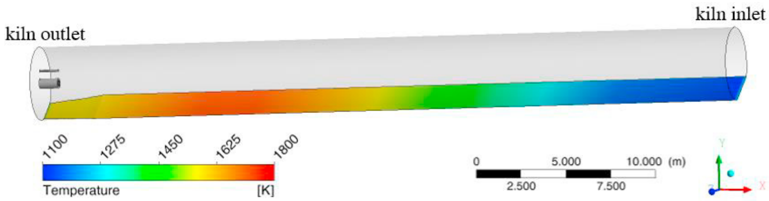

Fig. 4: Model of the rotary kiln with temperature profile for the static clinker bed.

Table 2: Composition and properties of the model RDF.

Fuel Components	Net Calorific Value (dry) [MJ/kg]	Mass-Fraction (ar) [%]	Particle Size Range, d_v* [mm]	Water [%]	Volatiles [%]	Fixed Carbon [%]
Fines	14.29	22	0.3-3.0	28.5	42.5	11.5
3D Plastics	38.19	24	2.4-10.3	1.0	97.9	0.0
2D Foil-sheets	37.07	24	1.5-9.1	0.9	93.9	0.0
Paper & Cardboard	14.50	18	2.5-14.3	25.7	53.2	10.5
Textiles	21.98	12	2.5-9.7	6.3	73.2	9.6
Fuel average	26.45	100	0.3-14.3	12.1	69.3	10.0

* d_v – equivalent spherical diameter

In total, 8 cases were simulated varying burner momentum, secondary air temperature, RDF particle size and RDF feed location (see Table 4). Axial and swirl burner momentum were calculated using the following eq. (1) & (2).

$$G_{ax} = \frac{\dot{m}_{sw} * w_{sw,ax} + \dot{m}_{tr+c} * w_{tr} + \sum \dot{m}_{ax} * w_{ax}}{\dot{Q}_{fuel}} \left[\frac{N}{MW}\right] \quad (1) \qquad G_{sw} = \frac{\dot{m}_{sw} * w_{sw,sw}}{\dot{Q}_{fuel}} \left[\frac{N}{MW}\right] \quad (2)$$

Here $\dot{m}_i$ are the mass flows of swirl (sw), axial (ax) and fuel transport air including the fuel (tr+c) and w_i the corresponding velocity components either in axial (ax) or swirl (sw) direction. $\dot{Q}_{fuel}$ is the thermal heat input at the main burner as in the reference Case 0.

We initially simulated two reference cases with relatively conservative burner settings, one for coal and one for RDF co-firing. The initial burner settings which are subject of the variations are listed in Table 3.

Table 3: Burner settings for reference cases.

Case	*Axial Momentum*	*Swirl Momentum*	*Sec. Air Temp*	*RDF feed location*	*Thermal heat input at main burner*
0	3.05 N/MW	0.80 N/MW	1300 K	-	38.72 MW
1	3.50 N/MW[1]	0.80 N/MW	1300 K	Central duct	38.72 MW

[1]RDF conveying air increases axial momentum

Table 4: Simulated cases and their variation.

Case	*Description of varied parameter*	*λ*
0	Reference case with 100 % lignite	1.32
1	Reference case with 64 % lignite and 36 % RDF	1.32
2	Case 1 with increased axial momentum by increasing jet-air (6.0 N/MW)	1.34
3	Case 1 with increased swirl momentum by increasing swirl-air (2.3 N/MW)	1.34
4	Case 1 with increased secondary air temperature (1450 K)	1.32
5	Case 1 with decreased particle sizes (particle mass reduced by 50 %)	1.32
6	Case 1 with RDF feed through separate lance 0.7 m above main burner	1.33
7	Case 6 with decreased particle sizes (particle mass reduced by 50 %)	1.33
8	Case 7 with increased swirl momentum at main burner (2.3 N/MW)	1.35

Based on these settings, variations were made and heat distribution and fuel burnout are analysed. Please note that in the cement industry further impacts of these variations could be of interest, e.g. emissions or the specific structure of the clinker, but in this paper we focus only on fuel burnout and local heat release. The variations made in the study, are based on empirical observations and on generally known guidelines for changing flame shapes and temperature distributions. Table 4 summarises the cases and their specific variation.

3.3. Results and Discussion

The calculated temperature distributions in a vertical plane through the kiln are shown in Figure 5. Case 0 depicts the temperature field for the lignite reference case while Case 1 shows the simulation results when replacing 36 % of the lignite with RDF. It can be seen that co-firing RDF in Case 1 leads to a narrower and shorter flame shape and significantly lower gas temperatures. Furthermore, a high temperature zone near the clinker bed at about half of the kiln length can be detected. This is due to the delayed ignition and slow thermal conversion of the relatively large RDF particles resulting in a large number of particles falling onto the clinker bed insufficiently converted. As the RDF particles which fall onto the clinker bed can lower the gas temperatures and can cause quality problems of the cement, these amounts should be kept as small as possible. The variations in this work were carried out with the intention to increase the burnout of the RDF particles and to achieve higher combustion temperatures.

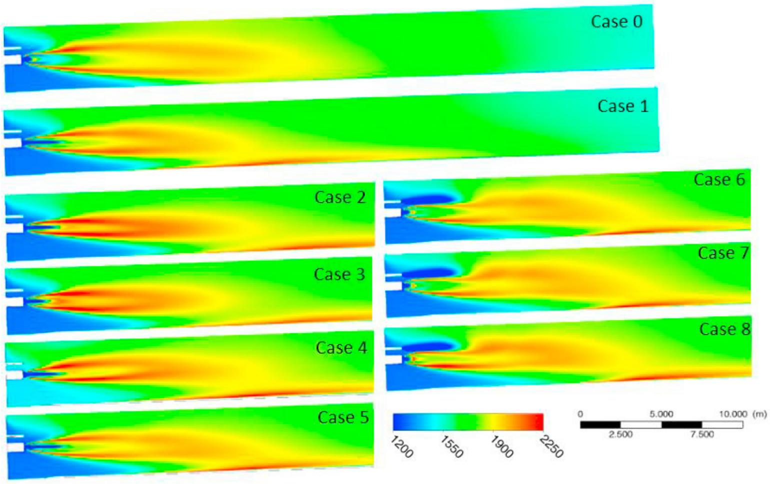

Fig. 5: Temperature distributions on the XY-plane for lignite and RDF co-firing cases.

Figure 6 shows the radially (mass flow weighted) averaged gas temperatures along the sintering zone, while Figure 7 illustrates the converted mass fractions of the different materials during their residence time in the gas phase (which result from analysing all particle trajectories before hitting the kiln walls or the clinker bed).

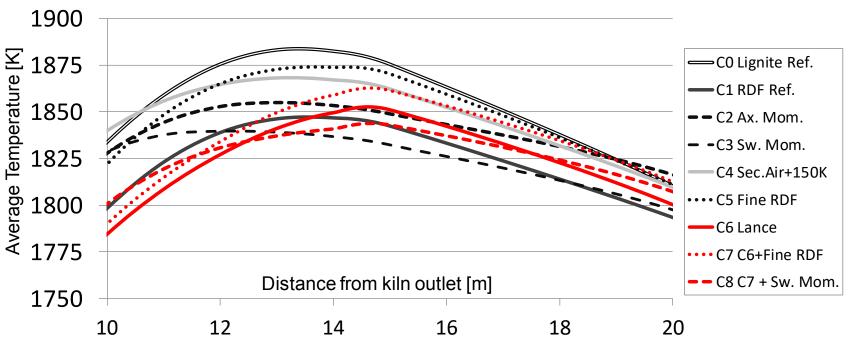

Fig. 6: Radially (mass flow-) averaged temperatures in the sintering zone for cases 0-8, burner at x=1 m.

For the reference case with RDF (Case 1), the radially averaged maximum temperature in the sintering zone is approximately 35 K lower compared to the lignite reference case. Regarding the particle burnout (Fig.7), it can be seen that P&C and 3D Plastics are the most problematic material fractions due to their overall larger particle size while providing a relatively small surface area and, in the case of P&C, high moisture content. 2D Foils and Textiles show a significantly better burnout due to their smaller particle sizes, low moisture and larger surface area. In the RDF reference case (C1), the total heat release of the RDF in the gas phase reaches only 40.8 %.

Figure 8 shows the averaged residence times of the particles in the gas phase before reaching the kiln walls or the clinker bed. For Case 1, relatively low residence times under 1.0 second reveal one significant cause for the poor RDF burnout.

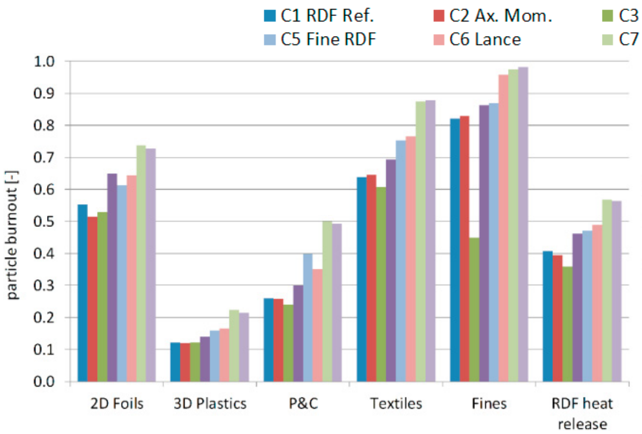

Fig. 7: Converted mass fraction of RDF before wall/bed contact.

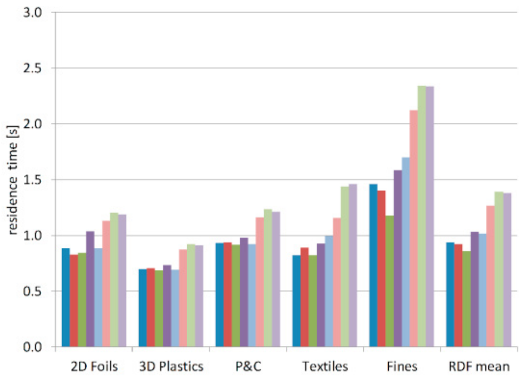

Fig. 8: Averaged residence times of RDF particles before wall/bed contact.

This insufficient burnout should usually result in a large temperature drop in the gas phase close to the sintering zone, however, our simplified particle boundary condition for particles reaching the material leads to a hot zone at the bottom of the kiln which increases the associated averaged gas temperatures (Fig. 6).

Changing burner momentum is a known method to influence the flame shape such as length, rotation or divergence. In Case 2 we increased the axial momentum by raising the jet air massflow. This setting leads to higher temperatures in the near burner region. The peak of the flame shifts more towards the burner which is often a beneficial effect for the sintering process. However, this setting has only a small effect to the overall particle burnout (-1 %) as residence times are slightly shorter. Increasing the swirl momentum in Case 3 results in a wider and even shorter flame with slightly lower peak temperatures. Interestingly, the RDF-burnout decreases significantly to 36 %, due to small particles which are directed towards the kiln walls, resulting in shorter residence times in the gas phase (see Fig. 8). This effect is less pronounced for the 3D, Textile and P&C Particles which are larger and more spherical in shape and, therefore, tend to follow their inertial trajectories. Increasing the secondary air temperature (C4) has significant influence on the overall temperature at the first half of the kiln (from burner), which leads to quicker ignition and to an increased heat release towards the burner. Regarding the particle burnout, this effect is smaller than initially expected (+6 %). The reason for that seems to be the relatively similar temperatures along the particle trajectories (which follow the center of the flame in the near burner region). For Case 5 we used a refined fuel where particle masses are reduced by 50 %. Using this fuel leads to a higher amount of released heat by +7 %. The average gas temperatures increase (+25 K at the peak) while flame length remains constant.

Next variations were made using a separate lance for RDF insertion. Results of Case 6 show marginal influence on the flame shape with just slightly lower near burner temperatures, caused by less central/axial air through the RDF channel at the burner. Regarding the RDF conversion, an improvement by +8.5 % of released heat can be identified. The residence times of the particles are longer (+30 %), and the particles pass through both edges of the flame envelope.

Injecting the finer RDF through the lance (Case 7) leads to an even higher heat release with 57 % and to a very similar temperature profile as in Case 6 with just slightly higher temperatures. Case 8 was carried out to examine a decoupling of the burner settings from the RDF feed through the lance. Hence, swirl air was increased similar to

Case 3 where particle burnout decreased noticeable. Comparing Case 7 and 8, the results of Case 8 show a higher average gas temperature up to 12 m, which is a similar effect as seen in Case 3. In contrast to Case 3, RDF heat release drops only by 0.7 % leading to 56.3 %, which is still a good improvement to 40.8 % in the reference case. This shows that using a separate RDF insertion does not only increase particle burnout but also offers the opportunity to improve flame shape by primary air settings independently with less (negative) influence on the particle trajectories.

4. Summary and Conclusion

In this paper, a numerical RDF modelling approach and its application to a case study on co-firing RDF in a cement rotary kiln is presented. The study was intended to reveal effects of operational settings on RDF combustion and resulting temperature distribution in the kiln.

In total, 9 simulations were performed, varying fuel properties, primary- and secondary air settings as well as particle sizes and fuel feed location. The RDF reference case was characterized by a relatively low RDF conversion in the gas phase (40.8 %), lower overall gas temperatures and a large amount of particles falling onto the clinker bed. According to the simulation results, adjustments which lead to favorable flame shapes do not automatically lead to a sufficient RDF burnout as varying primary air affects also particle trajectories and gas phase residence times. Insertion of the RDF through a separate lance showed good results for RDF burnout in the gas phase as residence times increased by over 30 %. This leads to an improvement of RDF burnout from 40.8 to 49.0 %. Reducing the particle masses by 50 % leads to further improvement by +8 % when the fuel is fed through the lance. A further advantage using a separate RDF injection is a decoupling from the burner settings, which can independently be adjusted to meet process requirements.

The case study shows a good applicability of the presented modelling procedure to analyse general impacts and effects of burner settings and plant set-up on RDF combustion and complements known measures for a successful plant operation while co-firing RDF.

Acknowledgements

Financial support by the German Federal Ministry for Economic Affairs and Energy (BMWi) through project 18862N of the German Federation of Industrial Research Associations “Otto von Guericke e.V. “. (AiF) gratefully acknowledged.

References

[1] Verein Deutscher Zementwerke (VDZ), Environmental Data of the German Cement Industry 2014, Düsseldorf, 2014.
[2] International Flame Research Foundation (IFRF), The Combustion of Pulverized Coal and Alternative Fuels in Cement Kilns – Results of the CEMFLAME-3 Experiments, IJmuiden, 1999.
[3] Forschungsinstitut der Zementindustrie, Optimierung der Verbrennung und Steigerung der Substitutionsrate von Sekundärbrennstoffen in der Hauptfeuerung von Drehofenanlagen der Zementindustrie, Abschlussbericht zum AiF-Forschungsvorhaben-Nr.: 15249 N, Düsseldorf, 2009.
[4] B. Krueger, S. Wirtz, V. Scherer, Measurement of drag coefficients of non-spherical particles with a camera-based method, Powder Technol. 278 (2015) 157–170. doi:10.1016/j.powtec.2015.03.024.
[5] W. Arnold, Erweiterte numerische Simulation der turbulenten , reagierenden Mehrphasenströmung in Calcinatoren der Zementindustrie, PhD Thesis, Ruhr-Universität Bochum, 2016.
[6] M. Kretschmann, Verbrennungsverhalten makroskopischer Einzelpartikel bei realistischen Feuerungsbedingungen, PhD Thesis, Ruhr-Universität Bochum, 2010.
[7] A. Hölzer, M. Sommerfeld, New simple correlation formula for the drag coefficient of non-spherical particles, Powder Technol. 184 (2008) 361–365. doi:10.1016/j.powtec.2007.08.021.
[8] M.A. Field, Rate of Combustion of Size-Graded Fractions of Char from a Low Rank Coal between 1200 K–2000 K, Combust. Flame. 13 (1969) 237–252.
[9] M.M. Baum, P.J. Street, Predicting the Combustion Behaviour of Coal Particles, Combust. Sci. Technol. 3 (1971) 231–243. doi:10.1080/00102207108952290.
[10] T. Bluhm-Drenhaus, Numerische Simulation der thermischen Zersetzung von Kunststoffen am Beispiel von Ersatzbrennstoffen in Calcinatoren der Zementindustrie, PhD Thesis, Ruhr-Universität Bochum, 2011.